Scaling of domain size during spinodal decomposition: Dislocation discreteness and mobility effects

Mikko Haataja[a)]
Department of Mechanical and Aerospace Engineering, Princeton University, Princeton, New Jersey 08544

Jennifer Mahon and Nikolas Provatas
Department of Materials Science and Engineering and Brockhouse Institute for Materials Research, McMaster University, Hamilton, Canada

Francois Léonard
Sandia National Laboratories, Livermore, California 94551

(Received 11 July 2005; accepted 8 November 2005; published online 12 December 2005)

In this letter, we examine the effects of discrete mobile dislocations on spinodal decomposition kinetics in lattice mismatched binary alloys. By employing a novel continuum model, we demonstrate that the effects of dislocation mobility on domain coarsening kinetics can be expressed in a unified manner through a scaling function, describing a crossover from $t^{1/2}$ to $t^{1/3}$ behavior.
 [DOI: 10.1063/1.2147732]

Spinodal decomposition is a technologically important solid-solid phase transformation which is often employed to strengthen alloys. During this process, domains of differing composition coarsen through bulk diffusion. A particularly interesting aspect of this process is the interaction between dislocations and the evolving microstructure in lattice mismatched alloys: The development of the spinodal microstructure is accompanied by a buildup of elastic coherency strains, which may be relaxed through the migration of misfit dislocations to the compositional interfaces.

In this letter, we introduce a phase-field model to describe discrete dislocations and their interaction with spinodal microstructures, and show that it captures basic dislocation behavior such as annihilation and migration to misfitting compositional interfaces. Then, we employ this model to simulate the time evolution of spinodal decomposition in binary alloys in the presence of dislocations and demonstrate that dislocation effects in intermediate and late-stage coarsening kinetics can be described through a single scaling function. That such a scaling function exists is nontrivial, as previous work employing a simpler continuum model of the dislocations has shown that dislocation mobility has unexpected effects on phase separation kinetics.[1]

We begin by describing the continuum phase-field model used in this study. The free energy is written as a sum of three terms

$$\mathcal{F} = \mathcal{F}_c + \mathcal{F}_{\mathbf{b}} + \mathcal{F}_{\text{coupl}}. \tag{1}$$

Here $\mathcal{F}_c$ is the free energy due to the spatially varying composition $c(\mathbf{r})$ (relative to the average alloy composition), given by

$$\mathcal{F}_c = \int d\mathbf{r}\left[-\frac{a}{2}c^2 + \frac{u}{4}c^4 + \frac{\varepsilon^2}{2}|\nabla c|^2\right], \tag{2}$$

where $a = a_0(T_c - T)$ with T as the temperature and T_c as the critical temperature, while a_0, u, and ε are positive constants. Dislocations are treated as continuum fields, and in two spatial dimensions they can be described by a continuous Burger's vector density $\mathbf{b}(\mathbf{r}) = [b_x(\mathbf{r}), b_y(\mathbf{r})]$. The dislocation free energy, $\mathcal{F}_{\mathbf{b}}$, is given by

$$\mathcal{F}_{\mathbf{b}} = \int d\mathbf{r}\left(\frac{\alpha}{2}|\mathbf{b}|^2 + \frac{1}{2Y}(\nabla^2\chi_d)^2 + \hat{c}_d\mathbf{b}^2(\mathbf{b}^2 - \hat{b}_0^2)^2 + \hat{W}^2/2[(\nabla b_x)^2 + (\nabla b_y)^2]\right), \tag{3}$$

where Y and $\chi_d(\mathbf{r})$ denote the Young modulus and Airy stress function due to dislocation strain fields, respectively. The first term in this equation describes dislocation core energies, where α is a constant. The second term accounts for the nonlocal elastic interactions (i.e., Peach–Koehler forces)[2] between the dislocations. Under mechanical equilibrium conditions, the Airy stress function satisfies (Ref. 3) $\nabla^4\chi_d = Y(\nabla_x b_y - \nabla_y b_x)$. The last two terms in Eq. (3), are introduced to impose a "discreteness" condition on $\mathbf{b}$ ($\mathbf{b}^2 = 0$ or $\mathbf{b}^2 = \hat{b}_0^2$) as well as to incorporate dislocation core interactions on length scales $\sim \hat{W}/(\sqrt{\hat{c}_d}\hat{b}_0^2)$, where $\hat{W}$, c_d, and $\hat{b}_0^2$ are positive constants. Finally, the interaction between the composition and the dislocations arises due to the dependence of the lattice constant on the composition and its coupling to the local compression $\nabla^2\chi_d$,[4]

$$\mathcal{F}_{\text{coupl}} = \eta\int d\mathbf{r}c\nabla^2\chi_d, \tag{4}$$

where η is proportional to the misfit.

The dynamics of the composition and dislocation density satisfy conservation laws. Upon converting to dimensionless variables through the replacements $c \to (|a|/u)^{1/2}c$, $\mathbf{r} \to (\varepsilon^2/|a|)^{1/2}\mathbf{r}$, $t \to (\varepsilon^2/\Gamma|a|)t$, $\mathbf{b} \to [|a|^3/(Y\varepsilon^2 u)]^{1/2}\mathbf{b}$, and $\chi_d \to (Y\varepsilon^4/u)^{1/2}\chi_d$, the dimensionless dynamical equation for the composition is given by

$$\frac{\partial c}{\partial t} = \nabla^2\frac{\delta\mathcal{F}}{\delta c} + \xi_c, \tag{5}$$

while the corresponding one for $b_x(\mathbf{r})$ can be written[5]

a)Electronic mail: mhaataja@princeton.edu

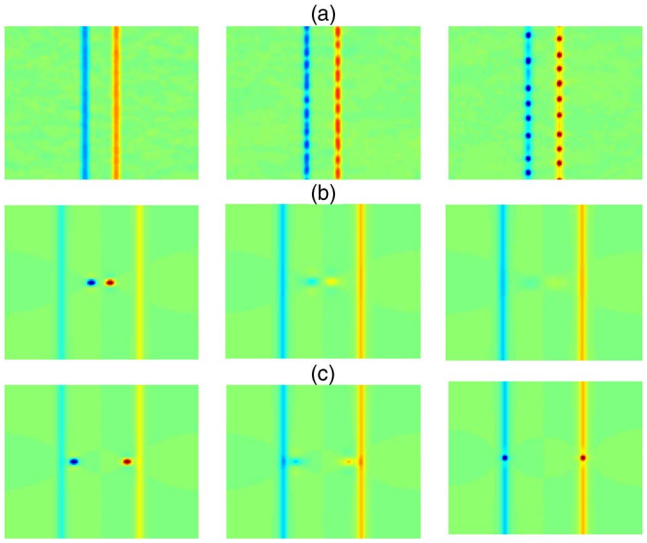

FIG. 1. (Color online) (a) Equilibrium dislocation density $b_y(\mathbf{r})$ in a stationary compositional morphology for $b_0=0.75$, $c_d=0.4$, $A=0.0025$ (left panel), $b_0=1.25$, $c_d=0.4$, $A=0.0025$ (middle), and $b_0=1.8$, $c_d=0.15$, $A=0.0025$ (right). Notice the emergence of localized dislocations as b_0 increases. (b) and (c) Panels depict the evolution of $b_y(\mathbf{r})$ starting form a dislocation pair with a small [(b)] or large [(c)] initial separation (time increases from left to right). The parameters employed were $b_0=1.8$, $c_d=0.15$, $A=0$. For small initial separations (b), dislocations annihilate each other, while for larger separations (c), they migrate in opposite directions to the compositional interfaces.

$$\frac{\partial b_x}{\partial t} = (m_g \nabla_x^2 + m_c \nabla_y^2)\frac{\delta \mathcal{F}}{\delta b_x} + \xi_{\mathbf{b}_x}; \tag{6}$$

the dynamical equation for b_y follows by replacing $b_x \rightarrow b_y$, $\nabla_y \rightarrow -\nabla_x$, and $\nabla_x \rightarrow -\nabla_y$ in Eq. (6). The dimensionless parameters are $\gamma = \eta Y^{1/2}/|a|^{1/2}$, $\epsilon = \alpha|a|/\varepsilon^2 Y$, $m_{c,g} = \Gamma_{c,g}\varepsilon^2 Y/\Gamma|a|^2$, $c_d = \hat{c}_d|a|^7/(u^2 Y^3 \varepsilon^6)$, $b_0 = \hat{b}_0[|a|^3/(Y\varepsilon^2 u)]^{-1/2}$, and $W = \hat{W}|a|/(Y^{1/2}\varepsilon^2)$. Here, Γ denotes the composition mobility while Γ_c and Γ_g are the dislocation mobilities in the climb and glide directions, respectively. Finally, thermal (Gaussian) fluctuations are represented by ξ_c and $\xi_{\mathbf{b}}$ with mean $\langle \xi_c \rangle = \langle \xi_{\mathbf{b}_x} \rangle = \langle \xi_{\mathbf{b}_y} \rangle = 0$ and variance $\langle \xi_c^2 \rangle = -2A\nabla^2 \delta(\mathbf{r}-\mathbf{r}')\delta(t-t')$ and $\langle \xi_{\mathbf{b}_x}^2 \rangle = \langle \xi_{\mathbf{b}_y}^2 \rangle = -2mA\nabla^2 \delta(\mathbf{r}-\mathbf{r}')\delta(t-t')$, where the dimensionless noise strength $A \equiv k_B T u/\epsilon^2|a|$.

We begin our exploration of the model by demonstrating that it naturally gives rise to simple discrete dislocation behavior. To this end, a stationary lamellar compositional morphology was set up, and the dynamical equations for $\mathbf{b}(\mathbf{r})$, Eq. (6) were numerically integrated on a 128×128 uniform grid with $\Delta x = 1.0$ using explicit Euler integration with time step $\Delta t = 0.005$. Spatial derivatives were obtained through finite differencing in real space and the Airy stress function $\chi(\mathbf{r})$ was resolved in Fourier space. The following parameters were employed in all of the simulations reported here: $\gamma = 1.0$, $\epsilon = 0.2$, and $W = 1.25$.

Let us first discuss the effect of b_0 on equilibrium dislocation configurations. As depicted in the panels in Fig. 1(a), increasing b_0 for fixed amount of misfit γ leads to the emergence of localized dislocations at the compositional interfaces. This results from the interplay between the elastic misfit (which determines the *average* dislocation density per unit length along the compositional interfaces) and the dislocation strength through b_0.

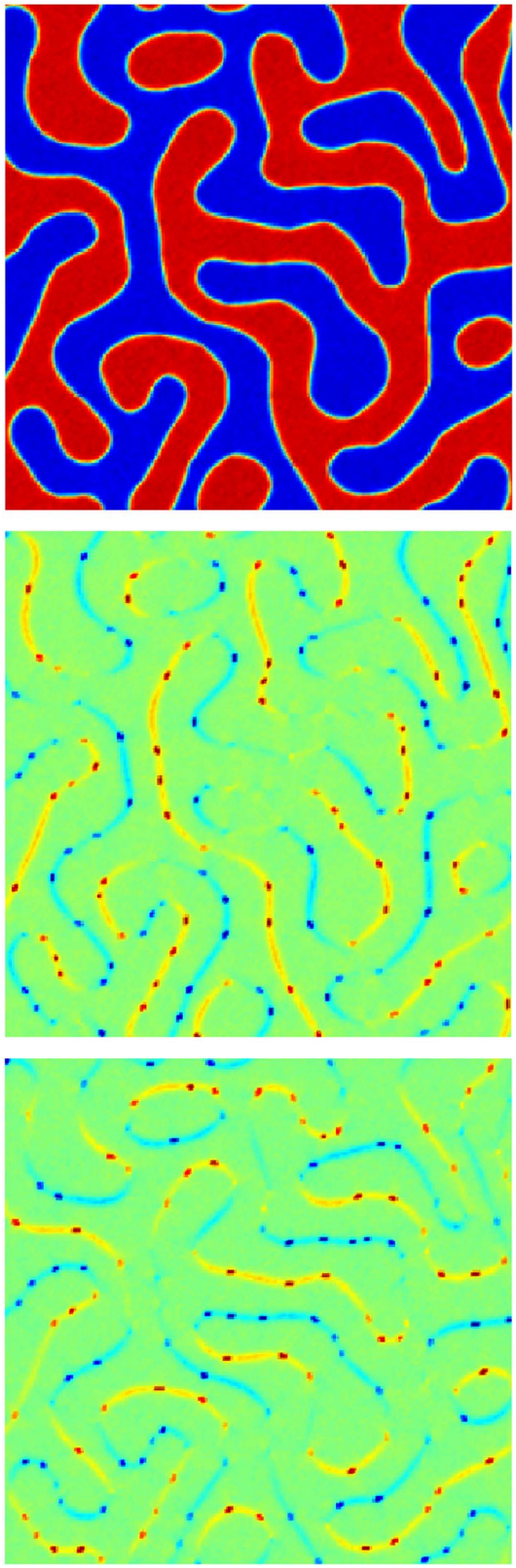

FIG. 2. (Color online) Typical configurations for composition $c(\mathbf{r})$ (top panel), $b_y(\mathbf{r})$ (middle panel), and $b_x(\mathbf{r})$ (bottom panel), during the phase separation process at dimensionless time $t=7500$ with dislocation strength $b_{x,y} = \pm b_0 = \pm 2.0$. Dark (light) shades represent large positive (negative) field values. Notice the accumulation of discrete dislocations at the compositional interfaces.

In order to further examine effective discrete dislocation behavior, a pair of dislocations with opposite signs were initially placed between the two compositional interfaces. In the absence of thermal fluctuations, we observed either annihila-

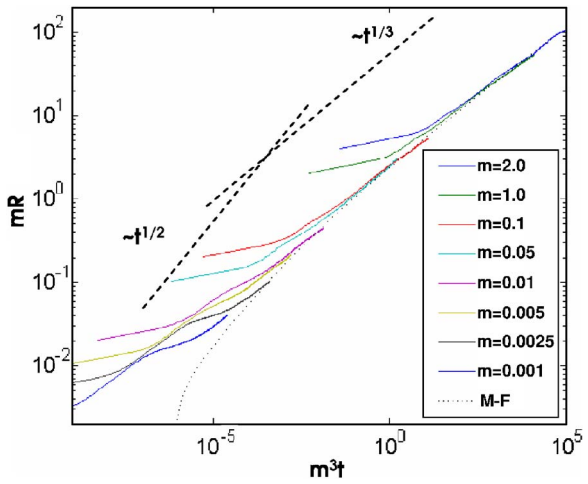

FIG. 3. (Color online) Scaled domain size mR for several values of the dislocation mobility as a function of m^3t. The mean-field scaling function has been shifted by a constant along the m^3t axis to clearly indicate scaling.

tion of the pair [if the initial separation between the dislocations was small—cf. Fig. 1(b)], or the migration of dislocations in opposite directions to the compositional interfaces [if the initial separation between the dislocations was sufficiently large—cf. Fig. 1(c)]. Indeed, this is what one would expect from a description based on discrete dislocations.

Having established the basic properties of our model, we now proceed to discuss the role of dislocations during phase separation. To this end, we simultaneously integrate the coupled dynamical Eqs. (5) and (6) on a 256×256 uniform grid. Figure 2 shows typical composition and dislocation configurations during the phase separation process at a dimensionless time $t=7500$. The data were obtained for the parameters $m_c=m_g=2.0$, $b_0=2.0$, $c_d=0.1$, and $A=0.0025$; the other parameters remain unchanged. For an Al-35 Zn alloy at $T=250\ ^\circ\mathrm{C}$, our system size corresponds approximately to 1 μm, while the maximum dimensionless time of Fig. 2 corresponds to a time of 200 h. As phase separation proceeds, dislocations migrate to compositional interfaces to relieve strain, and a strong coupling emerges between the motion of the domain walls and the dislocation mobility. This coupled motion of dislocations and composition leads to a modified behavior for the domain growth kinetics, which we now discuss.

As a quantitative measure of the domain growth kinetics, we have monitored the average domain size $R(t)=A/L(t)$ as a function of time, where A and $L(t)$ denote the total area and the total interface length in the system, respectively. As we have shown elsewhere,[1] dislocations with small mobility can lead to very slow domain growth rates while fast dislocations accelerate the coarsening kinetics. At late times, spinodal decomposition is always asymptotically accelerated in the presence of dislocations with nonzero mobility. We now show that discrete dislocation effects on the intermediate to late-time domain growth can be described by a single scaling function.

A mean-field expression for dislocation mobility effects on the average domain size $R(t)$ can be derived under the approximation $c_d=0$, $W=0$ and $\epsilon=0$,[1] and in the limit $mt\gg1$ can be expressed as

$$\frac{d(mR)}{d(m^3t)}\approx\frac{\sqrt{3}\sqrt{1+\gamma^2}}{8(mR)^2+\sqrt{3}mR\gamma^2\sqrt{1+\gamma^2}}. \tag{7}$$

Thus, Eq. (7) predicts a scaling solution for mR of the form

$$mR=f(m^3t,\gamma), \tag{8}$$

where the scaling function $f(x,y)$ behaves as

$$f(x,y)\sim\begin{cases}x^{1/2}y^{-1} & \text{intermediate } x\\ x^{1/3}(1+y^2)^{1/6} & \text{large } x.\end{cases} \tag{9}$$

In particular, the scaling form describes a crossover behavior from $R\sim t^{1/2}$ to the asymptotic behavior $R\sim t^{1/3}$. The existence of such a scaling function is demonstrated in Fig. 3, which plots mR versus m^3t obtained from simulations, and which clearly demonstrates data collapse on a universal curve at intermediate and late times for several values of dislocation mobility m. (The scaling function does not describe the early time behavior, since it was derived with the assumption of well-defined compositional domains with sharp interfaces.) The straight lines in Fig. 3 indicate a crossover between two scaling regimes with exponents of 1/2 and 1/3. Thus, mobile dislocations introduce a new scaling regime in spinodal decomposition, characterized by the behavior $R\sim t^{1/2}$.

In summary, we introduced a novel continuum model which captures the basic aspects of discrete dislocation motion. Numerical exploration of the model reveals that the effects of mobile dislocations on coarsening kinetics during spinodal decomposition can be described by a single crossover scaling function describing the evolution from a $t^{1/2}$ to a $t^{1/3}$ regime of growth.

One of the authors (N.P.) acknowledges support from the National Science and Engineering Research Council of Canada, as well as the Centre for Automotive Materials and Manufacturing. Another author (F.L.) acknowledges support from the Office of Basic Energy Sciences, Division of Materials Sciences, U.S. Department of Energy under Contract No. DE-AC04-94AL85000.

[1] M. Haataja and F. Léonard, Phys. Rev. B **69**, 081201 (2004).
[2] F. R. N. Nabarro, *Theory of Crystal Dislocations* (Dover, New York, 1967).
[3] L. Landau and E. M. Lifshitz, *Theory of Elasticity* (Pergamon, Oxford, 1986).
[4] F. Léonard and R. C. Desai, Phys. Rev. B **58**, 8277 (1998).
[5] M. Haataja, J. Müller, A. D. Rutenberg, and M. Grant, Phys. Rev. B **65**, 165414 (2002); **65**, 035401 (2002).